Acta Orthop. Scand. *58*, 545–548, 1987

A carbon chamber for vital microscopy of bone healing

Andrew Butterworth, Allen E. Goodship and Alan W. Preece[1]

We describe a carbon chamber implanted in the ulna of fowl. A window permitted daily microscopy of bone formation including observations of tetracyline labelling. The chamber could be heated to 5° above body temperature by 600 kHz radio frequency.

An optical method for studying bone-graft revascularization was described by Albrektsson (1978, 1980) and was further refined to study effects of electrical fields on bone capillaries (Nannmark et al. 1985). The techniques developed by Albrektsson and his co-workers involved the screwing of a cannulated titanium chamber through the rabbit tibia and observation, after surgical exposure, of invading vessels and bone inside a quartz glass "synthesis chamber."

We describe daily, in vivo photographic records of the changes within an artificial bone defect achieved by means of a carbon chamber.

Material and methods

The ulna of skeletally mature female domestic fowl (*Gallus gallus domesticus*) was chosen as an easily accessible non-weight-bearing bone.

The vitreous carbon percutaneous viewing port (Figures 1 and 2) was machined from a phenolic resin and then carbonized in a mildly reducing atmosphere at a temperature reaching a maximum of 1200°C. Polymeric vitreous carbons produced by this method have considerable tensile strength, of maximum 200 Mpa, and a high level of biocompatibility. It has been demonstrated that tissue, including bone, will form an intimate contact with carbon surfaces if the material has been manufactured with pores on its surface of several cell diameters in size (Tarvainen et al. 1985). Carbon will, however, produce a galvanic electrical current if used in combination with ferrous metals in an implant eventually leading to corrosion. For this reason all metallic parts were manufactured from surgical grade titanium. A 3.2-mm diameter, 0.35-mm thickness, glass disc was attached to the base of the carbon chamber with cyanoacrylate cement, thus forming the window between the living tissues and the external environment.

General anesthesia was induced by intravenous administration of 1.25 per cent sodium thiopentone and maintained after endotracheal intubation with halothane in oxygen on a semiclosed circuit. The feathers were then removed from the dorsal surface of the wing and the surgical site prepared with alcoholic chlorhexidine gluconate (Hibitane®, I.C.I.). Following a dorsal skin incision, the surface of the ulna metaphysis was exposed by blunt dissection. Two mounting holes for fixing the chamber in place were then drilled and tapped and the center point between these holes marked. At this marked point, the defect was generated by drilling through both dorsal and ventral cortices. The upper cortex was then enlarged to 2.7-mm diameter and the lower cortex tapped to 1.7-mm diameter through this large hole in preparation for insertion of a cannulated titanium screw containing an optic fiber light guide. The light guide was then screwed into the tapped hole through the upper cortex such that its head was positioned immediately below the endosteal

Comparative Orthopedic Research Group, Department of Anatomy, Bristol University, Park Row, Bristol, Avon, England, and [1]Radiotherapy Centre, Horfield Road, Bristol, Avon, England

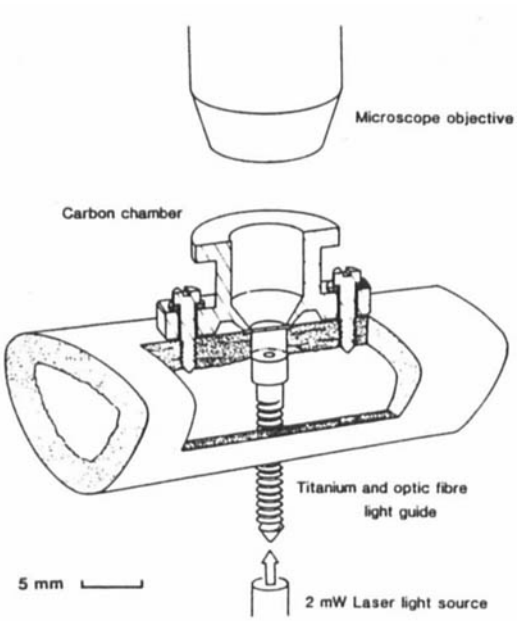

Figure 1. The carbon vital chamber is mounted on the ulnar surface so as to overlie an artificially generated circular defect, 2.7 mm in diameter. Illumination is achieved from above with ultraviolet light and from below via the cannulated light-guide, through which red laser light is passed.

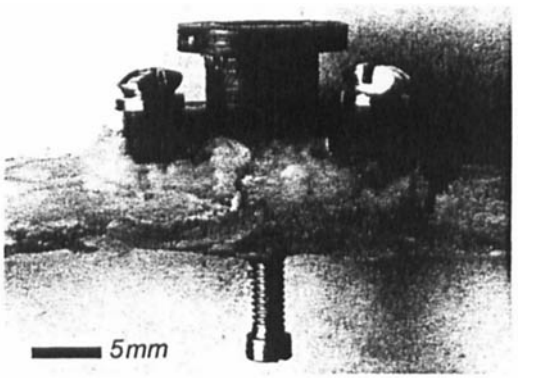

Figure 2. An excised ulna from a control animal after 1 month of implantation. Bone and callus have buttressed against the carbon surface to hold it quite firmly.

surface of the dorsal cortical defect. The defect in the cortex was 1.2-mm deep and 2.7-mm wide. The carbon chamber was then located so that the glass window was situated across the dorsal face of the defect, and was then fixed in this position with two short titanium cortex screws fitted with load-spreading washers (Figure 1).

At this stage a semiconductor microthermistor (U23-UD®, marketed by STC components, UK) was bonded to the chamber close to the edge of the defect. The leads to this thermistor, enclosed in 1-mm-bore PTFE tubing, were then passed subcutaneously to a small incision in the skin on the shoulder. The small connector to the thermistor leads was protected when the animal was in freedom by a small cloth pouch held in a bandage.

Oxytetracycline (Terramycin Q-50® Pfizer, oxytetracycline 50 mg/ml) was administered at a dose of 25 mg/kg daily by intramuscular injection. Observation of osteogenic changes within the circular defect were made possible using a Leitz Wetzlar Ortholux II® microscope fitted with Ploem system incident ultraviolet illumination of wavelength 400 nm.

Red laser light from a 2mW He-Ne laser was passed up the fiber-optic light-guide from below to illuminate the hematoma and fibrous tissues found within the defect during early stages of healing. This 2mW of laser light is a very low power input, and in practice there was no evidence that this low intensity illumination caused heating of the tissues within the defect. With the onset of mineralization, the laser illumination technique was superseded by fluorescence of newly accreted bone. The light levels available with both laser and fluorescence lighting methods were low, and it was necessary to use photographic exposure times of up to 20 seconds.

During vital microscope photography, the bird was seated on a contoured cradle and the right wing bearing the chamber was held gently, but firmly, with Velcro® tapes on a contoured micro-adjustable platform. The wing and chamber could then be precisely located under the microscope objective and be brought into focus. The bird was anesthetized with inhalation anesthetic (Halothane® in oxygen) for a short period during the photographic exposure.

A black and white photomontage of a typical healing sequence obtained by this method can be seen in Figure 3. Sketches of the progressive filling of the defect with bone mineral have been made to clarify the monochrome images.

It was recognized that the existing system comprising an electrically conductive carbon chamber and a metallic light-guide was ideally suited to the introduction of an electrical field to

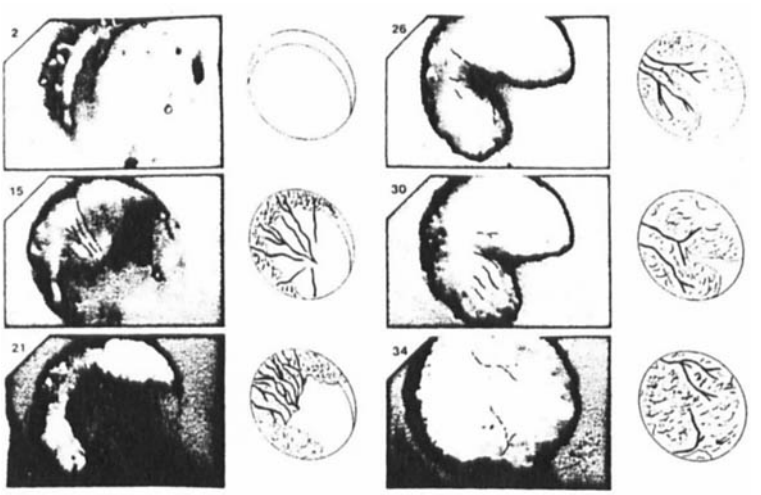

Figure 3. Photomontage of vital microscope photographs and schematic diagrams of healing events within a defect over a 34-day period. Vascular changes have been highlighted.
Day 2 – Hematoma obscures much of the defect. Sketch represents an empty disc, the unfilled defect.
Day 15 – Initial accretion of bone mineral has begun to occur. Capillaries are visible on surface of newly accreting bone and appear to focus on the center of the defect.
Days 12–30 – Progressive filling of defect with bone mineral occurs in close association with changes in the capillary network.
Days 30–34 – Further accretion of bone results in complete defect filling. By this time the surface capillary network has become very stable.

the defect. A method for generating a controlled temperature rise was devised using a localized current-field heating technique. A 600-kHz field was produced locally by using the carbon chamber as one pole of a radio-wave radiator, and the titanium lightguide as the other pole. The field was provided by a conventional surgical diathermy unit with a large current step-down stage to limit the output RF current to 100 mA. Heating in the RF field may be caused by capacitative effects causing rotation of dipoles within the tissue and by direct resistive heating. At 600-kHz, resistive heating is likely to predominate (Schwan & Piersol 1954). RF heating is used for destruction of tumors (Doss & McCabe 1976, Joseph et al. 1981), but has not been used in studies of bone formation. Initial tests in a thermally conductive phantom, which mimics the properties of tissue, indicated the magnitude of RF current that would be required to cause a local 5°C temperature rise. In vivo monitoring of the local temperature rise to body temperature plus 5°C was achieved by connecting the implanted thermistor to a digital thermometer. The local temperature could be controlled to within 1°C by altering the RF current generated by the diathermy unit; an RF current of between 30 and 80 mA at 6 V (r.m.s.) and 600 kHz (asymetrical sinusoidal) was suitable.

In a pilot study to assess the feasibility of the technique, a group of 12 birds were studied. Five birds were placed under a regime of local diathermic heating to 5°C above body temperature for 1 h in every 48 h over a period of 1 month. The remaining birds acted as controls. This control group and heated group demonstrated that the chamber and heating system could be successfully applied for a long-term investigation of osteogenic activity under thermal stimulation. The chamber and thermistor systems were found to be robust enough to withstand the rigors of long-term implantation in the mobile wing of an unrestrained bird.

Periodically, the entire chamber and defect locality was examined by radiography to detect any possible fracture at the defect site or damage to the chamber not visible externally. As carbon is radiolucent, the level of bone response was assessed by radiography without the chamber obscuring the site (Figure 4).

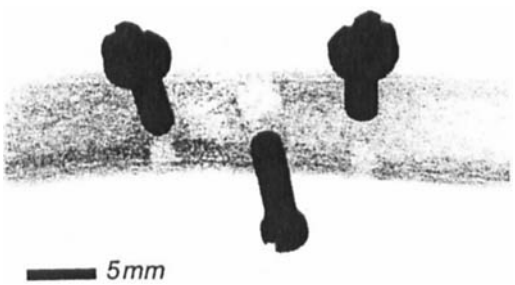

Figure 4. Radiograph (negative print) of ulna in the region of the chamber. The defect is visible as a light circular region between the upper fixing screws. Cannulated titanium light-guide is visible in the lower part of the photograph.

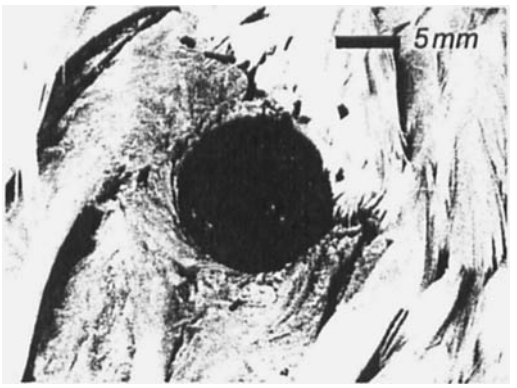

The chamber system was well tolerated by the animals and appeared to give them little irritation. No infection or exudation was noted around the skin-to-chamber interface after the initial period of healing, and in one bird epithelial growth was so profuse that the chamber became covered by skin and incorporated into the wing tissue. Such a tight carbon-to-skin interface may be seen in Figure 5.

Figure 5. External flange of the carbon percutaneous port as seen on the wing surface. The skin-to-chamber contact was tight and consistently free from exudation or visible infection.

References

Albrektsson T. In vivo studies of bone grafts. The possibility of vascular anastomoses in healing bone. Acta Orthop Scand 1980;51(1):9–17.

Albrektsson T, Albrektsson B. Microcirculation in grafted bone. A chamber technique for vital microscopy of rabbit bone transplants. Acta Orthop Scand 1978;49(1):1–7.

Doss J D, McCabe C W. A technique for localized heating in tissue: an adjunct to tumor therapy. Med Instrum 1976;10(1):16–21.

Joseph C D, Astrahan M, Lipsett J, Archambeau J, Forell B, George F W. Interstitial hyperthermia and interstitial iridium 192 implantation: a technique and preliminary results. Int J Radiat Oncol Biol Phys 1981;7(6):827–33.

Nannmark U, Buch F, Albrektsson T. Vascular reactions during electrical stimulation. Vital microscopy of the hamster cheek pouch and the rabbit tibia. Acta Orthop Scand 1985;56(1):52–6.

Schwan H P, Piersol G M. The absorption of electron energy in body tissue. Am J Phys Med 1954;33:371–404.

Tarvainen T, Patiala H, Tunturi T, Paronen I, Lauslahti. K, Rokkanen P. Bone growth into glassy carbon implants. A rabbit experiment. Acta Orthop Scand 1985;56(1):63–6.

Acknowledgements

The authors would like to thank the staff of both the Comparative Orthopedic Research Group, Department of Anatomy, and the Zoology Department, University of Bristol, for their invaluable help with this project.